River Flow 2014 – Schleiss et al. (Eds)
© 2014 Taylor & Francis Group, London, ISBN 978-1-138-02674-2

Sediment transport in steep channels with large roughness elements

T. Ghilardi, M.J. Franca & A.J. Schleiss
Laboratory of Hydraulic Constructions, Ecole Polytechnique Fédérale de Lausanne, Lausanne, Switzerland

ABSTRACT: Most sediment transport equations overestimate the bedload transport rate by several times when applied to mountain rivers. This is due to the fact that the presence of large relatively immobile boulders, which disrupt the flow, is generally not taken into account. Sediment transport in steep channels with boulders was herein investigated using 41 laboratory experiments carried out on a tilting flume for three slopes (S = 6.7%, 9.9%, and 13%). Sediment transport, mean flow velocities and morphology-describing variables were measured regularly during the experiments. The sediment transport capacity is clearly decreasing with dimensionless boulder distance and is better estimated in terms of critical discharge for incipient motion of mobile sediments than in terms of bed shear stress. A sediment transport formula based on excess discharge relative to a critical value, which depends not only on the channel slope but also on the boulder spatial density, is herein developed.

1 INTRODUCTION

Despite the importance of mountain rivers in the control of sediment supply to lowland mild-slope rivers (Yager et al., 2007), only a few studies were made on steep channels, mainly during the last two decades. These rivers are typically characterized by a stepped longitudinal profile and slopes ranging from 0.1% to almost 20% (Papanicolaou et al., 2004). The channel bed is composed of coarse mobile sediments, found in the pools or scouring holes downstream of steps, and by large immobile boulders (Papanicolaou et al., 2004, Yager et al., 2007), that can be found in steps spanning across the whole channel section (step-pool morphology) or arranged in a more irregular way (cascade morphology) (Montgomery and Buffington, 1997). These boulders are considered macro-roughness elements when the relative roughness (ratio between the roughness scale and the water depth) exceeds the unit value (Bathurst, 1978).

The presence of macro-roughness elements, which are enduring a significant part of the total shear stress and disrupting the flow by altering the channel roughness (Yager et al., 2007), impacts the sediment transport capacity of mountain rivers. This is due to the form drag caused by the boulders, which increases with their number, implying lower shear stresses available at the bed for sediment entrainment (Lenzi et al., 2006, Yager et al., 2007, Bathurst, 1978). Hence, the presence of boulders decreases the sediment transport capacity of rivers (Yager et al., 2007, Ghilardi, 2013). The effect of boulders is generally linked to the number of boulders per unit area, their cross section, the bed area occupied by them, the distance between boulders and a drag coefficient (Yager et al., 2007, Bathurst, 1978, Canovaro et al., 2007).

Most sediment transport formulae have the following general form:

$$q_b = \alpha\left(X - X_{cr}\right)^{\beta} S^{\gamma} \tag{1}$$

where q_b is the bedload transport, which may be expressed in different units depending on the equation ($m^3\ s^{-1}\ m^{-1}$, $kgs^{-1}\ m^{-1}$, or dimensionless; most often either the first or the last unit are used), α, β, and γ are empirical constants, S is the bed slope, X may be the liquid discharge q per unit width (Rickenmann, 1990), stream power ω per unit width (Bagnold, 1980), or, more commonly used, the dimensionless shear stress τ^* (Fernandez Luque and van Beek, 1976), being X_{cr} the corresponding critical value at which the bedload begins. The coefficient α is often expressed as a function of grain size diameters and liquid and solid densities. The exponent β is often set to 1 (Rickenmann, 1990), but can range up to 2 or 3 (Fernandez Luque and van Beek, 1976). γ has been found to vary between 1.5 and 2 by Rickenmann (1990) and found to be zero by Fernandez Luque and van Beek (1976).

Bed shear stress calculations, which may be used as X term in eq. (1), need a precise knowledge of the channel hydraulics, which has a high local variability in mountain rivers. Moreover, several authors highlighted the possible dependence of critical bed shear stress from the channel roughness and hiding effects due to the wide grain size distribution (Lenzi et al., 2006), the

channel gradient (Papanicolaou et al., 2004) and morphology (Church et al., 1998). On the other hand, the specific stream power (Bagnold, 1980), which quantifies the rate of loss of energy as water flows downstream, and thus the power potentially available for performing geomorphic work, can be approximated from such bulk channel properties as width and slope, combined with the river discharge. Gomez and Church (1989) showed that the stream power has a more significant correlation with sediment transport than any other hydraulic parameter. Rickenmann (1990) used another approach needing only gross channel properties: the discharge itself, with the corresponding critical discharge, which is solely related to the sediment grain size and the channel slope through a power law. Nevertheless, most formula do not predict sediment transport consistently well (Montgomery and Buffington, 1997, Yager et al., 2007).

The objective of this article is to preliminarily analyze the influence of boulders on sediment transport capacity and to make a first attempt in developing an equation expressing such influence. This is achieved through flume experiments where bedload, flow velocity, and bed morphology are assessed over time. Results herein presented are based on 35 experiments with boulders and 6 experiments without boulders, carried out for varying water and sediment discharges.

2 RESEARCH METHODS

2.1 *Experimental setup and procedure*

The impact of randomly distributed relatively immobile boulders on bedload fluctuations is investigated by means of laboratory experiments, carried out on a steep (longitudinal inclination of 6.7 to 13%), 8 m long (7 m usable) and 0.25 m wide, tilting flume at the Laboratory of Hydraulic Constructions (LCH) of the Ecole Polytechnique Fédérale de Lausanne (EPFL) (Fig. 1).

The boulders, with mean diameters D ranging between 1/3 and 1/2 of the flume width, were placed in the flume and partially covered by mobile sediments. Boulders are herein defined as elements that are not transported by the flow, although they may move up to several times their diameter during experiments, mainly due to the scour holes formed around them.

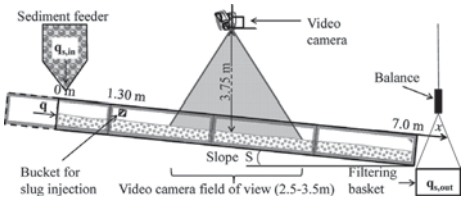

Figure 1. Sketch of the experimental setup.

A 0.2 m thick plane bed of poorly sorted sediments (d_{50} = 9.3 mm, d_{65} = 11.9 mm, d_{30} = 7.1 mm, d_{84} = 16.6 mm, and d_{90} = 19.0 mm) is prepared before the experiments and boulders are randomly placed into the flume, with an average distance λ, half buried into mobile sediments, which corresponds to a protrusion equal to approximately 30% of the equivalent sphere diameter approximately, since real stones are used in this research.

Water and poorly sorted sediments are constantly supplied at the flume inlet. Bedload at the channel downstream section, bulk flow velocities and morphological parameters are measured regularly during the experiments as described below.

Water discharge, fed constantly by the closed general pumping system of the laboratory, is controlled by an electromagnetic flow-meter (±0.01 l/s).

The poorly sorted sediments are constantly fed into the system by a calibrated sediment feeder situated upstream and recirculated during the experiment. A filtering basket suspended to a balance collects the sediments at the outlet where the weight (±1 kg) is measured every minute and the total average sediment transport rate (q_s) is calculated.

Average flow velocity (U) was measured every 15 minutes by means of dye-tracer injections and video analysis. A detailed description of the technique herein used is given in Ghilardi et al. (2013).

The protrusion (P) of four boulders is measured with a point gauge during the experiments, with a time interval of approximately 10 minutes (2 to 3 minutes per boulder, in a loop). The protrusion is then linearly interpolated to obtain a value every minute. An average protrusion value between the boulders (P_{av}) is then calculated for every minute of the experiment. The definition of boulder protrusion is illustrated in Figure 2a.

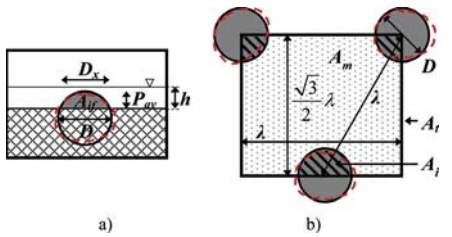

Figure 2. a) Schematic front view of one boulder, with the definition of the diameter D, the protrusion P_{av}, the reduced diameter D_x, and the frontal area A_{ij}; b) plan view with the definition of the distance between boulders λ, bed unit surface A_t, the immobile bed surface A_i, and the mobile surface A_m. The red dashed lines indicate the shape of real boulders.

Table 1. Experimental parameters and main bulk results. The symbols used to represent the experiments in Figure 3 to Figure 6 are given in the last column of the table. The filling of the symbols depends on λ/D (*inf* represents the tests without boulders, thus with an infinite distance), the shape on boulder diameter D and the contour line color on the flume slope S. For tests with *, boulder protrusion was measured at the end of the experiment. For tests with x, the number of hydraulic jumps was not counted. For tests with -, boulder surface was measured every 15 minutes, while for the others it was measured every minute.

	S (%)	λ/D (–)	D (m)	N_{Bs} (m^{-2})	q ($m^3\ s^{-1}\ m^{-1}$)	$q_{s,in} \times 10^{-3}$ ($m^3\ s^{-1}\ m^{-1}$)	$q_s \times 10^{-3}$ ($m^3\ s^{-1}\ m^{-1}$)	$\bar{U}$ (ms^{-1})	$P_{\overline{av}}$ (m)	HJ (m^{-2})	A_f/A_t (–)	A_{ff}/A_t (–)	Symb.
x-	6.7	2	0.075	45	0.0209	0.029	0.024	0.56	0.022	–	0.19	0.048	
-	6.7	2	0.075	45	0.0391	0.134	0.146	0.77	0.027	22	0.21	0.064	
x-	6.7	2	0.100	25	0.0228	0.057	0.065	0.71	0.024	–	0.17	0.036	
-	6.7	2	0.100	25	0.0372	0.134	0.139	0.70	0.029	14	0.19	0.048	
x-	6.7	2	0.100	25	0.0424	0.157	0.174	0.84	0.036	–	0.21	0.064	
x-	6.7	2	0.125	16	0.0228	0.063	0.075	0.64	0.037	–	0.19	0.049	
-	6.7	2	0.125	16	0.0352	0.134	0.137	0.70	0.040	13	0.20	0.054	
	6.7	3	0.075	20	0.0188	0.056	0.053	0.52	0.023	6	0.09	0.023	
x-	6.7	3	0.075	20	0.0212	0.091	0.104	0.63	0.031	–	0.10	0.034	
-	6.7	3	0.075	20	0.0238	0.134	0.140	0.70	0.033	12	0.10	0.037	
-	6.7	3	0.100	11	0.0177	0.056	0.061	0.49	0.024	4	0.07	0.016	
-	6.7	3	0.100	11	0.0233	0.134	0.124	0.55	0.031	8	0.09	0.023	
x*-	6.7	3	0.100	11	0.0240	0.139	0.156	0.67	0.025	–	0.08	0.017	
-	6.7	3	0.125	7	0.0236	0.101	0.112	0.60	0.043	4	0.09	0.026	
-	6.7	3	0.125	7	0.0235	0.134	0.119	0.60	0.054	5	0.10	0.035	
x*-	6.7	3	0.125	7	0.0240	0.156	0.171	0.90	0.032	–	0.08	0.017	
-	6.7	5	0.075	7	0.0168	0.056	0.057	0.53	0.017	2	0.03	0.005	
-	6.7	5	0.075	7	0.0222	0.134	0.131	0.58	0.029	4	0.03	0.011	
-	6.7	5	0.100	4	0.0162	0.056	0.056	0.42	0.031	3	0.03	0.008	
	6.7	5	0.100	4	0.0183	0.094	0.088	0.55	0.028	2	0.03	0.007	
-	6.7	5	0.100	4	0.0223	0.134	0.135	0.57	0.046	4	0.04	0.014	
	6.7	5	0.125	2	0.0156	0.056	0.060	0.52	0.027	1	0.02	0.004	
-	6.7	5	0.125	2	0.0208	0.134	0.150	0.63	0.061	2	0.04	0.014	
-	6.7	inf	–	0	0.0148	0.056	0.065	0.35	0.000	0	0.00	0.000	*
	6.7	inf	–	0	0.0159	0.094	0.100	0.58	0.000	0	0.00	0.000	*
-	6.7	inf	–	0	0.0162	0.134	0.119	0.49	0.000	0	0.00	0.000	*
x-	6.7	inf	–	0	0.0204	0.186	0.151	0.72	0.000	0	0.00	0.000	*
	9.9	3	0.100	11	0.0131	0.094	0.089	0.38	0.021	2	0.07	0.013	
	9.9	3	0.100	11	0.0146	0.136	0.143	0.53	0.035	5	0.09	0.027	
	9.9	3	0.100	11	0.0166	0.192	0.198	0.61	0.036	5	0.09	0.028	
	9.9	inf	–	0	0.0112	0.094	0.088	0.40	0.000	0	0.00	0.000	*
	13	2	0.100	25	0.0128	0.146	0.168	0.41	0.017	8	0.13	0.022	
	13	3	0.075	20	0.0109	0.146	0.172	0.36	0.010	3	0.05	0.007	
	13	3	0.100	11	0.0107	0.146	0.145	0.28	0.016	2	0.05	0.009	
	13	3	0.100	11	0.0114	0.192	0.199	0.37	0.013	2	0.05	0.007	
	13	3	0.100	11	0.0124	0.236	0.254	0.38	0.025	5	0.08	0.017	
	13	3	0.100	11	0.0118	0.236	0.261	0.37	0.021	3	0.07	0.013	
	13	3	0.125	7	0.0104	0.146	0.165	0.27	0.035	3	0.08	0.019	
	13	4	0.075	11	0.0118	0.236	0.266	0.34	0.013	2	0.03	0.006	
	13	5	0.100	4	0.0104	0.146	0.168	0.37	0.024	2	0.03	0.006	
	13	inf	–	0	0.0106	0.192	0.216	0.28	0.000	0	0.00	0.000	*

Hydraulic Jumps (*HJ*) are counted manually based on visual observation every 15 minutes. This parameter is an indicator of the amount of energy dissipation and morphological variety, since hydraulic jumps generally appear downstream of the protruding boulders.

The bed surface occupied by boulders parallel to the river bed (A_{Bs}), called in short "boulder surface", is obtained by means of video analysis.

The frontal area of boulders (A_{if}) and the bed surface occupied by boulders (A_i) can be calculated as defined in Figure 2. The boulder diameter is reduced (D_x) to account for the boulder protrusion, as defined in eq. (2). It corresponds to the diameter of the circle at the surface of the mobile sediments. This definition is helpful for the calculation of boulder frontal area (A_{if}, (eq. (4)), Fig. 2a) and bed parallel area (A_i, (eq. (5), Fig. 2b). A unit bed surface is defined A_t (eq. (3)), similarly to Yager et al. (2007), depending on the average distance λ between randomly placed boulders (Fig. 2b). In a unit bed surface, only one boulder is present, as shown in Figure 2b, thus for a unit bed area A_t, the frontal surface occupied by boulders correspond to A_{if} and bed area occupied by boulders corresponds to A_i. The mobile bed surface A_m is calculated as the difference between the total and the immobile bed surface (eq. (6)).

$$D_x = 2\sqrt{P_{av}(D - P_{av})} \tag{2}$$

$$A_t = \sqrt{3}\lambda^2/2 \tag{3}$$

$$\begin{cases} A_{if} = \left[D/2\left(D\sin^{-1}(D_x/D) - D_x\right) + D_x P_{av} \right]/2 \\ \quad \text{if } P_{av} < 0.5\,D \\ A_{if} = \pi D^2/4 - \left[D/2\left(D\sin^{-1}(D_x/D) - D_x\right) + D_x P_{av} \right]/2 \\ \quad \text{if } P_{av} \geq 0.5\,D \end{cases} \tag{4}$$

$$\begin{cases} A_i = \pi {D_x}^2/4 & \text{if } P_{av} < 0.5\,D \\ A_i = \pi D^2/4 & \text{if } P_{av} \geq 0.5\,D \end{cases} \tag{5}$$

$$A_m = A_t - A_i \tag{6}$$

The imposed equilibrium condition between liquid and solid discharge (couple $q_s - q$) is such that boulders are still relatively visible at average sediment transport. The total average sediment transport rate has to be within ±15% of the sediment supply at the end of the experiment. More details on the experimental setup are given in Ghilardi (2013).

Table 1 presents the configuration of the experiments, characterized by slope S, dimensionless boulder distance λ/D, equivalent boulder diameter D, number of boulder per square meter N_{Bs}, water discharge q per unit width, and sediment supply $q_{s,in}$ per unit width. The main bulk results, averaged during the whole experiment are also presented. This includes the total average sediment outlet q_s, the mean flow velocity $\bar{U}$, the average boulder protrusion $\overline{P_{av}}$, the number of hydraulic jumps per square meter *HJ*, the immobile bed surface per unit surface A_i/A_t (eq. (3) and (5)), and the boulder frontal area per unit surface A_{if}/A_t (eq. (3) and (4)).

3 RESULTS AND DISCUSSION

3.1 *Influence of the liquid discharge*

In Figure 3, presenting the sediment transport capacity as a function of the discharge, the tests are clearly grouped by slope. For a given liquid discharge, higher bedload transport occurs at steeper slopes. A trend as a function of boulder dimensionless distance (λ/D) is also visible in Figure 3. This is most evident on the smallest slope (S = 6.7%),

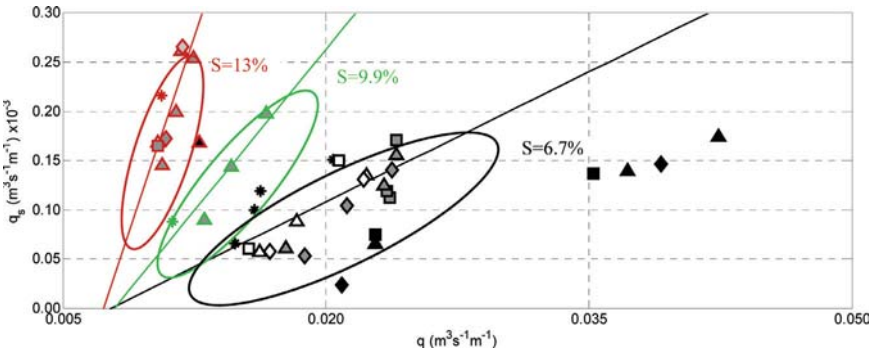

Figure 3. Average sediment transport capacity q_s (m^3 s^{-1} m^{-1}) as a function of water discharge q (m^3 s^{-1} m^{-1}). Data are grouped by channel slope and linear trend lines are given for each slope, without taking into account the experiments with λ/D = 2. The symbols used are presented in Table 1.

where the highest number of tests with different boulder densities was carried out.

Experiments without boulders show a higher sediment transport capacity, indicating that with boulders a greater liquid discharge is needed to transport the same amount of sediments. The transport capacity decreases for decreasing dimensionless distances λ/D (boulder more closely packed), as observed by Yager et al. (2007). Relatively small differences are observed between $\lambda/D = 5$ and $\lambda/D = 3$. For a dimensionless distance of 2, the transport capacity decreases abruptly, especially for higher discharges. As mentioned by Yager et al. (2007), the impact of boulders rapidly decreases with increasing distances, and this also confirms Canovaro et al. (2007) observations about the higher effect of boulder geometry on shear stress for $\lambda/D \simeq 2$ (i.e. $\Gamma = 0.2$, in their spatial parameter). This may be related to the characterization of the flow around boulders changing from an isolated roughness to a wake interference flow (Canovaro et al., 2007). In the latter case, the interference between boulders becomes more important and more energy can be dissipated.

By further analyzing the data for each value of λ/D on the smallest slope ($S = 6.7\%$, Fig. 3), the influence of the diameter becomes also visible. For a given sediment discharge, slope, and λ/D, the data are aligned with increasing discharge for decreasing diameters. This effect may be due to the boulder diameter itself or to the number of boulders, or both of them, since for a given λ/D the number of roughness elements increases with the diameter. Although the same trend as a function of λ/D and D is visible on the steepest slope, the impact of the boulder configuration becomes almost negligible. Here again, the experiment carried out for $\lambda/D = 2$ is the only one detaching from the trend line, confirming the possible change in boulder interaction and flow behavior, going from isolated roughness elements to wake interference between boulders (Canovaro et al., 2007).

In Figure 4 it can be seen in detail how sediment transport capacity is affected by the flume slope for a given boulder configuration ($\lambda/D = 3$ and $D = 0.100$ m, Fig. 4a) and by the distance among boulders for a given diameter and a given flume slope ($D = 0.100$ m and $S = 6.7\%$, Fig. 4b). Figure 4a shows a clear linear relation between the liquid and solid discharge data for the tested longitudinal inclinations of the flume. The slope of this linear trend increases with S, for $\lambda/D = 3$ and $D = 0.100$ m, which is consistent with the observation for the entire dataset presented in Figure 3, with the exception of experiments characterized by a dimensionless distance of $\lambda/D = 2$. In Figure 4, the discharge corresponding to the zero-crossing of the vertical axis is the critical discharge (q_{cr}) for the onset of bedload. Figure 4a indicates that it increases with slope, which is consistent with the observations made by Rickenmann (1990).

Figure 4b indicates that the influence of dimensionless distance λ/D exists, but it is secondary when compared to the slope effect. As it can be seen, q and q_s within the same boulder density (λ/D) are linearly linked. For $\lambda/D = 3$ and $\lambda/D = 5$ the slope of this trend is similar to that of experiments without boulders, and generally q values increase with decreasing λ/D, for the same q_s value. For the larger boulder density ($\lambda/D = 2$), the slope of the linear relation between q and q_s is smaller.

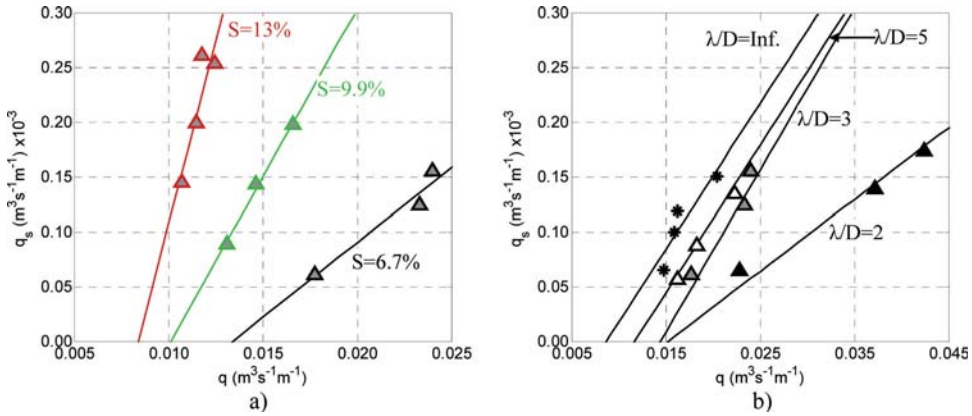

Figure 4. Average sediment transport capacity q_s ($m^3\ s^{-1}\ m^{-1}$) as a function of water discharge q ($m^3\ s^{-1}\ m^{-1}$). a) Effect of the flume slope for a given boulder configuration ($\lambda/D = 3$ and $D = 0.1$ m). b) Effect of dimensionless distance λ/D for a given slope ($S = 6.7\%$) and a given boulder diameter ($D = 0.1$ m), and for experiments without boulders. The linear trend lines are shown for each data set. The symbols used are presented in Table 1.

The results presented in Figure 4b indicate that the correlation between λ/D and the values of liquid and solid discharge is probably non-linear and increases exponentially with decreasing distances between boulders. The critical discharge for beginning of motion slightly increases with decreasing dimensionless boulder distance. For small dimensionless distances ($\lambda/D = 2$), the effect of boulders increases with the solid discharge (trend line slope smaller than for the experiments without boulders), going from an increase of liquid discharge of approximately 50% for the smaller solid discharge with respect to the test without boulders, up to about 85–100% for the highest solid discharge. More precisely, for a sediment supply of about 0.136×10^{-3} m^3 s^{-1} m^{-1} the corresponding liquid discharge is increased of 10–15% for $\lambda/D = 5$, 25–35% for $\lambda/D = 3$, and up to 100% for $\lambda/D = 2$ compared to the reference test without boulders. This clearly indicates again that the roughness elements have to be taken into account when evaluating the critical discharge for the beginning of sediment motion in a mountain river with boulders.

In Figure 4, the critical discharge seems to vary linearly with λ/D and as a power law with the flume slope S. A similar trend for critical discharge as a function of the channel slope was found on steep flumes by Rickenmann (1990), with the critical discharge dependent on the slope to the power –1.12. For a 6.7% channel slope, the very same value of 0.0087 m^3 s^{-1} m^{-1} is obtained from the linear regression presented in Figure 4b and from Rickenmann (1990) critical discharge formula. The critical discharge, and thus the bedload transport capacity, is probably also a function of the boulder diameter or protrusion, as suggested by the data alignment (tendency to a decrease in transport capacity for an increasing diameter) in Figure 3.

A formula for dimensionless critical discharge is inferred, through a non-linear least square solver, as a function of the slope S and the boulder dimensionless distance λ/D:

$$q_{cr}^{*} = q_{cr} \Big/ \sqrt{g d_{50}^{3}} = S^{-0.46} \left(1 - D/\lambda\right)^{-0.7} \tag{7}$$

where q_{cr} is a discharge per unit width (m^3 s^{-1} m^{-1}) and q_{cr}^{*} its dimensionless form (Lenzi et al., 2006). The determinant coefficient of eq. (7) is $R^2 = 0.87$.

3.1.1 *Influence of the bed shear stress*

The bed shear stress is a variable generally used as parameter to estimate bedload. Figure 5 presents the sediment transport as a function of the total bed shear stress τ^{*} (eq. (8), Fig. 5a) and the drag shear stress on mobile sediments τ_m^{*} (eq. (9), Fig. 5b)

$$\tau^{*} = \rho g R_h S \Big/ \left[\left(\rho_s - \rho\right) g d_{50}\right] \tag{8}$$

where ρ and ρ_s (kgm^{-3}) are the liquid and solid density respectively, and R_h (m) is the hydraulic radius.

$$\tau_m^{*} = 0.5 \rho C_m U^2 \Big/ \left[\left(\rho_s - \rho\right) g d_{50}\right] \tag{9}$$

where C_m (–) is a drag coefficient and U (ms^{-1}) is the mean flow velocity (Yager et al., 2007, Scheingross et al., 2013).

The correlation between sediment transport and the shear stress seems weak. Nevertheless, according to Figure 5a, bedload capacity tends to increase with total bed shear stress τ^{*}, which is clearly higher

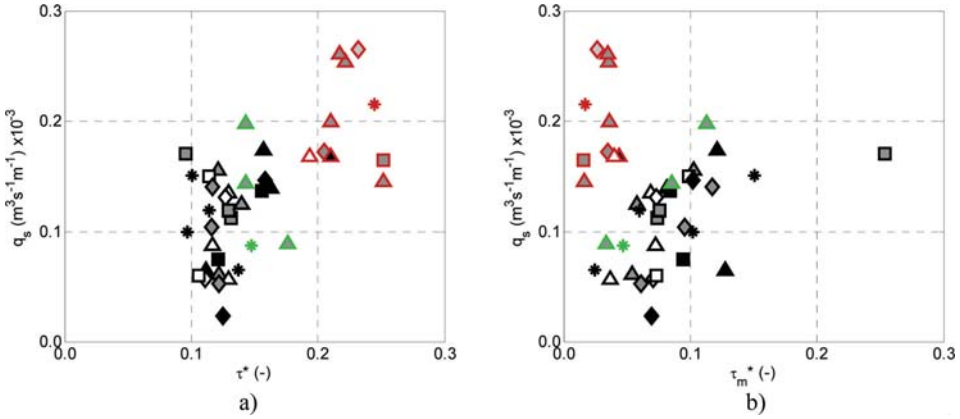

Figure 5. Measured sediment transport q_s (m^3 s^{-1} m^{-1}) as a function of a) the dimensionless total bed shear stress τ^{*} (–) and b) the dimensionless drag shear stress acting only on the mobile sediments τ_m^{*} (–). The symbols used are presented in Table 1.

on steep slopes. However, no link to the presence of boulders can be observed in the data.

According to Yager et al. (2007) and Lenzi et al. (2006), only the part of the total shear stress acting on mobile sediments, i.e. τ_m^*, contributes to sediment transport. In eq. (9), the drag coefficient C_m is calculated with the Variable Power Equation of Ferguson (2007) as suggested by Scheingross et al. (2013), with a relative submergence defined as R_h/d_{50}, where R_h is the hydraulic radius (Ghilardi (2013) for more details). The bed drag shear stress τ_m^* (Fig. 5b) is clearly higher on smaller slopes and the transport capacity visibly tends to increase with the drag on mobile sediments. Nevertheless no trend of the drag shear stress as a function of boulder density is visible. The bed drag shear stress acting on mobile sediments is smaller than the total bed shear stress (Fig. 5a), confirming the observations of Yager et al. (2007) and Canovaro et al. (2007).

In order to estimate a critical bed shear stress (for both the total bed shear stress and the drag shear stress acting on the mobile sediments), several formulae (Papanicolaou et al., 2004, Ferro, 1999, Lamb et al., 2008) and several constant values were applied the data. These equations calculate the critical bed shear stress as a function of either the flume slope or the relative roughness. For both, the total bed shear stress and the drag bed shear stress acting on mobile sediments, a constant critical value supplied the best estimate ($\tau_{cr}^* = 0.091$ for the total bed shear stress and $\tau_{m,cr}^* = 0.007$ for the drag bed shear stress acting on mobile sediments).

3.2 *Development of a sediment transport equation considering boulder influence*

Hereinafter, a sediment transport formula with the form of eq. (1) is developed by testing both liquid discharge and bed shear tress (total and drag reduced) as parameter identified as X in the equation.

As shown by the previous discussion of results, the sediment transport capacity is clearly linked with the presence of boulders. As suggested by Yager et al. (2007), a correction factor taking into account the presence of these may thus be introduced in the sediment transport formula. Several correction factors depending on the morphological parameters are hereafter tested, individually or in a combined fashion (Table 2): A_m represents the mobile bed surface, calculated according to

Table 2. Coefficients of the tested sediment transport formulae and percentage error (in the last column; in bold the best results). The line is gray is further used as sediment transport equation (eq. (11)).

				Correction factor (C_i)				
	Base parameters			A_m/A_t	$1-A_{ij}/A_t$	$1-(D-2P_{av})/(\lambda)$	$(\lambda-D)\lambda^{-1}$	
Crit. param (X_{cr}^*)	α	β	γ	ε_1	ε_2	ε_3	ε_4	Err (%)
q_{cr} (eq.(7))	4.69	0.49	2.10	–	–	–	–	*20.6*
	4.79	0.52	2.10	0.46	–	–	–	*20.4*
	4.82	0.53	2.10	–	1.68	–	–	*20.4*
	4.65	0.50	2.11	–	–	–0.19	–	*20.5*
	4.68	0.49	2.10	–	–	–	–0.02	*20.6*
	5.54	**0.70**	**2.27**	**5.96**	**–**	**–**	**–1.62**	***17.6***
	5.30	0.65	2.20	–	10.78	–	–0.77	*19.1*
$\tau_{cr} = 0.091$	0.37	0.00	0.94	–	–	–	–	*32.1*
	0.42	–0.03	1.05	–0.63	–	–	–	*32.0*
	0.56	–0.09	1.26	–	–4.85	–	–	*31.3*
	0.45	0.01	0.97	–	–	0.48	–	*31.7*
	0.37	–0.01	0.96	–	–	–	–0.05	*32.1*
	0.68	–0.06	1.25	–3.30	–	–	0.79	*31.4*
	1.09	**–0.12**	**1.53**	–	**–13.45**	–	**0.81**	***29.9***
$\tau_{m,cr}^* = 0.007$	1.98	0.23	1.34	–	–	–	–	*29.6*
	1.98	0.23	1.34	0.02	–	–	–	*29.6*
	1.89	0.21	1.36	–	–2.02	–	–	*29.4*
	3.15	0.24	1.47	–	–	0.70	–	*28.7*
	2.27	0.24	1.36	–	–	–	0.13	*29.5*
	3.43	0.24	1.52	–2.99	–	–	0.92	*28.8*
	3.65	**0.22**	**1.58**	**–**	**–10.37**	**–**	**0.83**	***27.9***

equation (6); A_{if} is the frontal area occupied by boulders per unit surface calculated using equation (4); $1-(D-2P_{av})/\lambda$ represents the wetted perimeters between boulders; $(\lambda - D)\lambda^{-1}$ is an indicator of the boulder spatial density. The correction factors are introduced as shown in equation in (10) to calculate the dimensionless sediment transport q_s^*. One or more correction factors C can be applied to the sediment transport formula to account for the presence of boulders. The dependence of the bedload to these factors may or may not be linear, thus the optimal power coefficient ε is searched for each coefficient.

$$q_s^* = \alpha(X^* - X_{cr}^*)^{\beta} S^{\gamma} C_1^{\varepsilon_1} \ldots C_n^{\varepsilon_n} \quad (10)$$

The constant coefficient α, is often dependent on sediment and fluid density, gravitational acceleration, and grain size (Rickenmann, 1990). The variation of these parameters was however not assessed in the present research and α was determined through regression analysis of the data as well.

In eq. (10), the critical dimensionless value X_{cr}^* for incipient motion is taken either as the critical discharge (q_{cr}^*, eq. (7)), the total critical bed shear stress ($\tau_{cr}^* = 0.091$, Fig. 5a), or the critical drag bed shear stress ($\tau_{m,cr}^* = 0.007$, Fig. 5b). Table 2 presents the bedload transport formulae herein developed, showing the constants α, β, γ, and ε_i obtained with a non-linear least square algorithm, for each form of formula. The percent error of the sediment transport estimation is given in the last column.

Table 2 shows that for all the tested excess values ($X^* - X_{cr}^*$), the equations obtained without the correction factors to account for the presence of roughness elements are less performing than those using a correction factor.

Moreover, equations based on the excess of discharge perform better than those based on the bed shear stress. This is not surprising since a clearer link between the liquid discharge and the bedload was already noticed in Figure 3, when compared to the relation between the bedload and the bed shear stress (total and drag) in Figure 5.

For equations based on the total bed shear stress ($\tau^* - \tau_{cr}^*$), the excess shear stress has an almost zero value for the coefficient. Only the slope seems to be relevant and the estimation error is of 32.1%. Coefficients obtained for the correction factors often present illogical values and only slightly decrease the estimation error, meaning that using total bed shear stress may not be adequate to parameterize the sediment transport in presence of boulders, as already argued by Yager et al. (2007).

Results obtained for equations based on the drag bed shear stress are more reasonable, although the excess shear stress is considered through a low coefficient (approximately 1/4) and presents a high bedload capacity estimation error (29.6%). As suggested by Yager et al. (2007) and Lenzi et al. (2006), only the shear stress acting on mobile sediments participate to the bedload transport.

When estimating the bedload transport with the excess discharge using only the base parameters (no correction factors), the error obtained with a variable critical discharge (eq. (7)) is of 20.6%. As shown Table 2, the improvement obtained when introducing correction factors is limited and is given by the following combination: $((\lambda - D)\lambda^{-1})^{-1.62}(A_m/A_t)^{5.96}$, giving an error of 17.6%. The fact that only a small improvement of bedload estimates is obtained when introducing a correction factor considering the presence of boulders as shown in equation (10) in a bedload formula using eq. (7) suggests that the influence of boulders is observed mainly on the incipient motion of sediments, for the range of sediment and liquid discharge used in the present research.

Thus, in a first attempt to develop a sediment transport equation accounting for the presence of relatively immobile boulders, we suggest using a bedload formula based on critical discharges calculated according to eq. (7). The following equation is proposed for sediment transport capacity calculation on steep slopes in the presence of boulders:

$$q_s^* = 4.69 S^{2.10} \sqrt{q^* - q_{cr}^*} \quad (11)$$

where q^* (–) is the dimensionless liquid discharge, q_{cr}^* (–) is the dimensionless critical discharge calculated according to equation (7) and depending

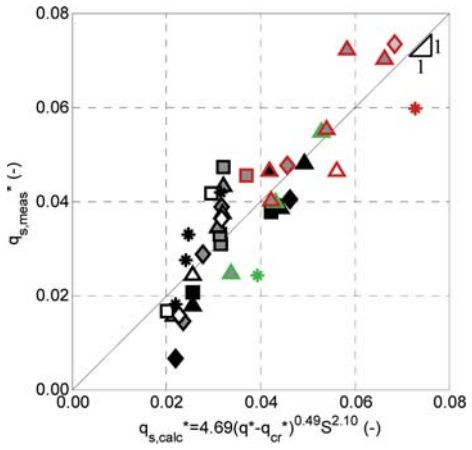

Figure 6. Measured sediment transport capacity against calculated sediment transport capacity (eq. (11)). The black line indicates the unitary slope curve. The symbols used are presented in Table 1.

from the flume slope and the dimensionless distance between boulders λ/D, where D (m) the boulder diameter, λ (m) the distance between boulders, and S (–) is the channel slope.

In Figure 6 the estimation results based on equations (7) and (11) are compared to the measured data. No trend as a function of neither boulder configuration nor slope is observed.

4 CONCLUSIONS

The sediment transport capacity in a steep channel with boulders was analyzed through a dataset of 41 experiments carried out with varying flume slopes and boulder configurations (combination of boulder dimensionless distance and diameter) for several sediment supply conditions.

It is underlined that the channel slope has the strongest impact on the transport capacity, namely in what concerns the critical discharge for beginning of motion. However, it is also clearly shown that the sediment transport decreases with dimensionless boulder distance λ/D. The impact of the boulder diameter D is also pointed out; for a given λ/D and a given channel slope, the transport capacity seems to decrease with boulder diameter. When the dimensionless distance corresponds to $\lambda/D = 2$, the transport capacity decreases drastically, especially for higher discharges, probably due to a change in the flow pattern, going from a flow between isolated roughness elements to a wake interference flow among boulders.

This paper underlines that, in steep channels, sediment transport formulae based on excessive discharge perform better than those based on excessive bed shear stress. The herein developed sediment transport equation (11), based on excess discharge calculation according equation (7), supplies accurate bedload estimation. The portion of boulder exposed to the flow (protrusion) is yet not included in this preliminary equation and further work is ongoing in order to develop an approach including it.

ACKNOWLEDGMENTS

The present study is supported by the Swiss Competence Center for Environmental Sustainability (CCES) of the ETH domain under the APUNCH project and the Swiss Federal Office of Energy (SFOE).

REFERENCES

Bagnold, R.A. 1980. An Empirical Correlation of Bedload Transport Rates in Flumes and Natural Rivers. *Proceedings of the Royal Society of London. Series A, Mathematical and Physical Sciences,* 372, 453–473.

Bathurst, J.C. 1978. Flow resistance of large-scale roughness. *Journal of the Hydraulics Division,* 104, 1587–1603.

Canovaro, F., Paris, E. & Solari, L. 2007. Effects of macro-scale bed roughness geometry on flow resistance. *Water Resources Research,* 43.

Church, M.A., Hassan, M.A. & Wolcott, J.F. 1998. Stabilizing self-organized structures in gravel-bed stream channels: Field and experimental observations. *Water Resources Research,* 34, 3169–3179.

Ferguson, R.I. 2007. Flow resistance equations for gravel- and boulder-bed streams. *Water Resources Research,* 43.

Fernandez Luque, R. & Van Beek, R. 1976. Erosion and transport of bed-load sediment. *Journal of Hydraulic Research,* 14, 127–144.

Ferro, V. 1999. Friction factor for gravel-bed channel with high boulder concentration. *Journal of Hydraulic Engineering,* 125, 771–778.

Ghilardi, T. 2013. *Sediment transport and flow conditions in steep rivers with large immobile boulders*. PhD., Ecole Polytechnique Fédérale de Lausanne (EPFL).

Ghilardi, T., Franca, M.J. & Schleiss, A.J. 2013. Bulk velocity measurements by video analysis of dye tracer in a macro-rough channel. *Measurement Science and Technology,* In press.

Gomez, B. & Church, M.A. 1989. An assessment of bed load sediment transport formulae for gravel bed rivers. *Water Resources Research,* 25, 1161–1186.

Lamb, M.P., Dietrich, W.E. & Venditti, J.G. 2008. Is the critical Shields stress for incipient sediment motion dependent on channel-bed slope? *Journal of Geophysical Research,* 113.

Lenzi, M.A., Mao, L. & Comiti, F. 2006. When does bedload transport begin in steep boulder-bed streams? *Hydrological Processes,* 20, 3517–3533.

Montgomery, D.R. & Buffington, J.M. 1997. Channel-reach morphology in mountain drainage basins. *Geological Society of America Bulletin,* 109, 596–611.

Papanicolaou, A.N., Bdour, A. & Wicklein, E. 2004. One-dimensional hydrodynamic/sediment transport model applicable to steep mountain streams. *Journal of Hydraulic Research,* 42, 357–375.

Rickenmann, D. 1990. *Bedload transport capacity of slurry flows at steep slopes* PhD, ETH Zürich (Swiss Federal Institute Of Technology Zurich).

Scheingross, J.S., Winchell, E.W., Lamb, M.P. & Dietrich, W.E. 2013. Influence of bed patchiness, slope, grain hiding, and form drag on gravel mobilization in very steep streams. *Journal of Geophysical Research: Earth Surface,* 118.

Yager, E.M., Kirchner, J.W. & Dietrich, W.E. 2007. Calculating bed load transport in steep boulder bed channels. *Water Resources Research,* 43, W07418.